



Effect of reference objects on the accuracy of digital implant impressions in partially edentulous arches

Vygandas Rutkūnas^{1*}, Darius Jegelevičius¹, Justinas Pletkus¹, Liudas Auškalnis¹, Mykolas Akulauskas², Tan Firat Eyüboğlu³, Mutlu Özcan⁴, Agnė Gedrimienė¹

¹Department of Prosthodontics, Institute of Odontology, Faculty of Medicine, Vilnius University, Vilnius, Lithuania

²Biomedical Engineering Institute, Kaunas University of Technology, Lithuania, Department of Electronics Engineering, Kaunas University of Technology, Lithuania

³Department of Endodontics, Faculty of Dentistry, Istanbul Medipol University, Istanbul, Turkey

⁴University of Zurich, Clinic of Masticatory Disorders and Dental Biomaterials, Center for Dental Medicine, Zurich, Switzerland

ORCID

Vygandas Rutkūnas

<https://orcid.org/0000-0001-5740-4573>

Darius Jegelevičius

<https://orcid.org/0000-0002-5999-7744>

Justinas Pletkus

<https://orcid.org/0000-0003-3132-2646>

Liudas Auškalnis

<https://orcid.org/0000-0001-6113-3753>

Mykolas Akulauskas

<https://orcid.org/0000-0002-1984-9931>

Tan Firat Eyüboğlu

<https://orcid.org/0000-0002-0308-9579>

Mutlu Özcan

<https://orcid.org/0000-0002-9623-6098>

Agnė Gedrimienė

<https://orcid.org/0000-0003-3377-9447>

Corresponding author

Vygandas Rutkūnas

Department of Prosthodontics,
Institute of Odontology, Faculty of
Medicine, Vilnius University,
Zalgirio str. 115, LT-08217 Vilnius,
Lithuania

Tel +37068755661

E-mail vygandasr@gmail.com

Received May 24, 2024 /

Last Revision August 26, 2024 /

Accepted October 22, 2024

The study was supported by the Lithuanian Business Support Agency grant Nr. J05-LVPA-K-01-0055 and DIGITORUM research team registration number "MTTP SK".

PURPOSE. This study assesses the impact of additional reference objects (RO) on the trueness and precision of distance and angle measurements between scan bodies in digital scans with four different intraoral scanners (IOS) in partially edentulous models. **MATERIALS AND METHODS.** Maxilla models (Frasaco, Frasaco GmbH, Tettngang, Germany) with one (3-U) and two (4-U) missing posterior teeth were 3D printed and fitted with dental implants and scan bodies. Four intraoral scanners (Primescan (Dentsply Sirona, Charlotte, NC, USA) (PS), Trios 3 (3Shape) (T3), Trios 4 (3Shape) (T4), and CS3600 (Carestream Dentistry) (CS)) captured digital implant impressions with and without additional RO. Scans were aligned and assessed for distance and angulation measurements between scan bodies. Statistical analyses compared trueness and precision across model groups using the Student t-test and Welch's ANOVA. **RESULTS.** CS consistently showed the highest distance values across IOS devices in both the 4-U and 3-U models ($P < .05$), both with and without RO. The distance values were not considerably affected by the presence of RO ($P > .05$), except for a few isolated cases in the PS and CS groups of 3-U models. When measuring angles, CS usually showed greater values than the other IOS devices, especially when RO was present both in the 4-U and 3-U variants ($P < .05$). **CONCLUSION.** The influence of additional reference objects on accuracy varies with different scanner types, irrespective of edentulous area length. [J Adv Prosthodont 2024;16:302-10]

KEYWORDS

Accuracy; Partially edentulous; Precision; Reference objects; Trueness

INTRODUCTION

New methods for clinical practice are made possible by the ongoing advance-

© 2024 The Korean Academy of Prosthodontics

© This is an Open Access article distributed under the terms of the Creative Commons Attribution Non-Commercial License (<https://creativecommons.org/licenses/by-nc/4.0>) which permits unrestricted non-commercial use, distribution, and reproduction in any medium, provided the original work is properly cited.

ment of digital technology, but the accuracy of digital implant impressions is still the primary concern in dentistry. The accuracy of 3D digital implant scanning is comparable to traditional implant impressions, according to the most recent systematic reviews and meta-analyses; however, these findings are primarily based on *in vitro* research.^{1,2}

Some of the parameters that may affect the accuracy of the digital implant impression (DII) include the implant number and its placement on the dental arch,³ the distance and angulation between the implants,^{4,5} the scan body design,⁶ and the scanning technique.⁷ Long edentulous regions separating implants in partially or completely edentulous jaws may potentially interfere with the scanning process due to potential image stitching issues. To increase scanning quality and speed, various types of additional reference objects (RO) fixed at edentulous locations were suggested for use.⁸⁻¹¹ Nonetheless, research utilizing several forms of RO yields inconsistent findings about the influence of RO on the precision of digital scanning.^{8,11,12}

Trueness and precision are characteristics of scanning accuracy. Trueness is the measurement's ability to match the actual value, whereas precision is the scanner's ability to yield consistent findings when multiple measurements of the same object are done.³ It is challenging to select an appropriate intraoral scanner (IOS) due to the wide range of manufacturers offering different models, each with varying performance and indications, even if advances in digital technologies have made superior alternatives to traditional approaches available.

The aim of this study was to evaluate the effect of additional reference objects on the digital implant impression accuracy, measuring the differences in angulation and distance between scan bodies in two partially edentulous models (simulating situation of three- and four-unit two-implant-supported bridge) when four different IOS were used. The null hypothesis stated that (1) using a different IOS does not influence the trueness and precision of the distance and angle values, and (2) using an RO does not affect the trueness and precision of the distance and angle values among the IOS devices.

MATERIALS AND METHODS

Using the Frasaco model (Frasaco GmbH, Tett nang, Germany) as a guide, two different types of maxilla models were manufactured using the Asiga Max UV (Asiga, Sydney, version 1.2.11) 3D printer. Since the right side of the initial model (4-U) lacked both premolars and molars, dental implants measuring 4.1 mm in diameter from Straumann (Basel, Switzerland) were placed in place of the first premolar, which was positioned straight, and the second molar, which was positioned 20° mesially inclined. Additionally, two implants were placed in the second partially edentulous model (3-U) in the locations of the second molar (tilted 20° mesially) and second premolar (straight). A cordless electronic screwdriver (iSD900, NSK) was used to attach scan bodies (CARES RC Mono scan body, Straumann) at a torque of 15 Ncm to the implants (Fig. 1). The models were then scanned using a Nikon Altera 10.7.6 (Nikon Metrology) reference scanner to create reference scans.

Primescan (Dentsply Sirona, version 5.0.1) (PS), Trios 3 (3Shape, version 1.18.2.10) (T3), Trios 4 (3Shape, version 19.2.2) (T4), and CS3600 (Carestream dentistry, version 3.1.0) (CS) IOS were used to capture DII ten times (n = 10) for each model without the use of RO. The scanning sequences were implemented following the instructions provided by each manufacturer and the IOS manuals. The scans were made for full



Fig. 1. Models simulated three-unit or four-unit two-implant-supported (BLT Implant, Ø 4.1- mm RC; Straumann, Basel, Switzerland) fixed partial denture situation. Distal implants were tilted mesially 20°.

arch to be as close to clinical workflow as possible. Subsequently, edentulous portions were attached with tablets (approximately $\text{Ø}2 \times 1 \text{ mm}$) of hardened glass-ionomer cement (Fuji Plus, GC, Tokyo, Japan) to create extra RO between implants on the top of alveolar ridge. RO tabs were fixed to the model using glass-ionomer cement (Fuji Plus, GC). All models were then scanned again using four different IOS. For further analysis, the scanning data were exported in the standard tessellation language (STL) format. Using the best-fit alignment technique and Geomagic Control X 2018 (3D Systems Corporation, Morrisville, NC, USA) software, every scan was accurately aligned on the reference scan.

To align CAD models of scan bodies to the scanned surfaces of scan bodies, distance and angulation characteristics between scan bodies were measured. The intersection of a predetermined center axis and the scan body's bottom plane (9 mm below the top surface of the scan body) was used to determine the scan body's center point. The measurement was made of the distance between the two scan bodies' center locations. The bottom plane of the scan body was used to better represent the expected misfit at the implant-abutment interface. The angle between two vectors that represented the scan bodies' axes in three dimensions was used to calculate the angulation of the bodies (Fig. 2).

All measured parameters had their trueness and precision calculated, and the results were compared

across the model groups with and without RO. The statistical software Matlab 2020a (The MathWorks Inc., Natick, MA, USA) was used to conduct the statistical study.

The Student two-sample t-test was used for each scanner to test for differences between models with and without RO to estimate statistically significant differences between measurements. A significance level of 0.05 was chosen. Welch's ANOVA was used to compare the outcomes of each model among scanners because the homogeneity of variance condition was not met. For post-hoc analysis, the Games-Howell test was employed.

RESULTS

In terms of trueness, the highest distance deviation (μm) in 4-U models was observed in CS (194.8 ± 167.5), followed by T3 (43.1 ± 18.6), T4 (33.4 ± 18.1) and PS (26.3 ± 19.2), respectively. The difference between CS and PS was statistically significant ($P = .048$), while the differences among the other IOS devices were insignificant ($P > .05$). With the involvement of RO in 4-U models, the highest distance values were observed in CS (193.2 ± 167.0), followed by T4 (37.1 ± 14.9), T3 (32.0 ± 18.0), and PS (20.4 ± 11.6), respectively. The difference between CS and PS was statistically significant ($P = .04$), while the differences among the other IOS devices were insignificant ($P > .05$). The presence of RO did not affect the distance results in 4-U models

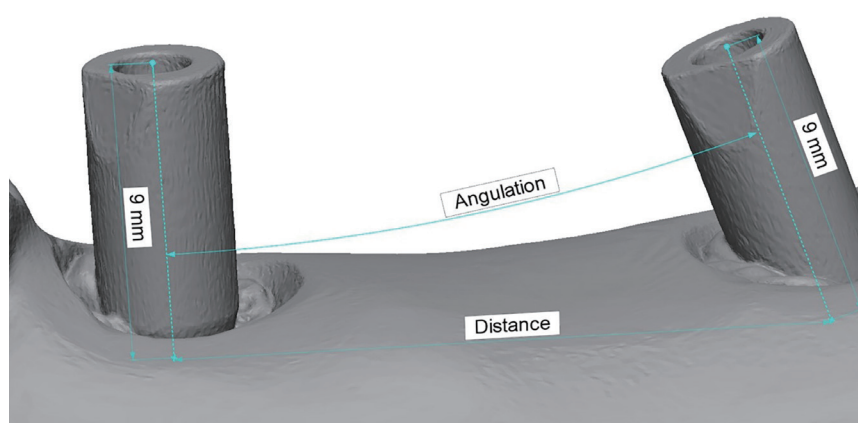


Fig. 2. Representation of distance and angulation measurements between the scan bodies.

Table 1. The trueness of mean distance and angle values with their standard deviation in 4-unit models with or without RO with their respective *P* values

	Distance, μm mean \pm std	<i>P</i> *	Angle, $^{\circ}$ mean \pm std	<i>P</i> *
PS 4-U	26.3 \pm 19.2 ^b	.42	0.22 \pm 0.04 ^a	.03
PS 4-URO	20.4 \pm 11.6 ^x		0.18 \pm 0.04 ^{xy}	
CS 4-U	194.8 \pm 167.5 ^a	.98	0.41 \pm 0.29 ^{ab}	.91
CS 4-URO	193.2 \pm 167.0 ^y		0.40 \pm 0.25 ^x	
T3 4-U	43.1 \pm 18.6 ^{ab}	.19	0.12 \pm 0.09 ^b	.72
T3 4-URO	32.0 \pm 18.0 ^{xy}		0.14 \pm 0.10 ^y	
T4 4-U	33.4 \pm 18.1 ^{ab}	.62	0.14 \pm 0.09 ^{ab}	.93
T4 4-URO	37.1 \pm 18.1 ^{xy}		0.14 \pm 0.12 ^y	

PS: Primescan, CS: CS 3600, T3: Trios 3, T4: Trios4, 4-U: 4 unit (length of restoration), 4-URO: 4 unit with reference objects, a,b: The different letters show statistically significant differences between 4-U group within each column. x,y: The different letters show statistically significant differences between the 4-URO group within each column.

**P* < .05

in any of the IOS devices significantly in terms of trueness (*P* > .05) (Table 1).

In terms of trueness, the highest angle ($^{\circ}$) value in 4-U models was observed in CS (0.41 \pm 0.29), followed by PS (0.22 \pm 0.04), T4 (0.14 \pm 0.09), and T3 (0.12 \pm 0.09), respectively. The difference between PS and T3 was statistically significant (*P* = .003), while the differences among the other IOS devices were not statistically significant (*P* > .05). With the involvement of RO, in 4-U models, the highest angle values were observed in CS (0.40 \pm 0.25), followed by PS (0.18 \pm 0.04), T4 (0.14 \pm 0.12), and T3 (0.14 \pm 0.10), respectively. The differences between CS-T3 (*P* = .047) and CS-T4 (*P* = .049) were statistically significant, while there was no significant difference among the other IOS devices. The presence of RO presented a statistically significant difference in only the PS group (*P* = .03), while the presence of RO created no significant difference for the other IOS devices (*P* > .05) (Table 1).

In terms of trueness, in 3-U models, CS (128.2 \pm 86.0) presented the highest distance deviation values, significantly different from all the other IOS devices, followed by PS (9.7 \pm 5.5, *P* = .01), T4 (8.9 \pm 5.2, *P* = .01) and T3 (8.6 \pm 4.6, *P* < .01), respectively. The differences among the other IOS devices were not statistically significant (*P* > .05). With the presence of RO in 3-U models, CS (42.7 \pm 27.4) presented the highest distance values, significantly different from all the

other IOS devices, followed by T4 (8.9 \pm 5.2, *P* = .02), T3 (10.0 \pm 9.1, *P* = .02) and PS (4.0 \pm 2.9, *P* < .01), respectively. The differences among the other IOS devices were not statistically significant (*P* > .05). In 3-U models, the presence of RO created a statistically significant difference in the PS group (*P* = .01) and CS group (*P* = .008) in terms of the trueness of distance values. RO presence presented no significant effect with the other IOS devices in 3-U models (*P* = .05) (Table 2).

In terms of trueness, the highest angle ($^{\circ}$) value in 3-U models was observed in CS (0.33 \pm 0.14), followed by T4 (0.22 \pm 0.12), T3 (0.12 \pm 0.04), and PS (0.08 \pm 0.05), respectively. Only the differences between CS and PS (*P* = .003), CS and T3 (*P* = .007), and T4 and PS (*P* = .02) were statistically significant. With the presence of RO in 3-U models, T4 (0.22 \pm 0.08) presented the highest angle values, followed by CS (0.19 \pm 0.14), T3 (0.14 \pm 0.08) and PS (0.11 \pm 0.04), respectively. Only the difference between PS and T3 was statistically significant (*P* = .01) (Table 2).

In terms of precision, the highest distance (μm) in 4-U models was observed in CS (143.4 \pm 83.3), followed by PS (17.5 \pm 9.6), T4 (15.3 \pm 8.1) and T3 (14.7 \pm 10.2), respectively. Only the differences between CS and PS (*P* = .007), CS and T3 (*P* = .006), and CS and T4 (*P* = .006) were statistically significant. With the involvement of RO, in 4-U models, the highest distance

Table 2. The trueness of mean distance and angle values with their standard deviation in 3-unit models with or without RO with their respective *P* values

	Distance, μm mean \pm std	<i>P</i> *	Angle, $^{\circ}$ mean \pm std	<i>P</i> *
PS 3-U	9.7 \pm 5.5 ^b	.01	0.08 \pm 0.05 ^a	.14
PS 3-URO	4.0 \pm 2.9 ^x		0.11 \pm 0.04 ^x	
CS 3-U	128.2 \pm 86.0 ^a	.008	0.33 \pm 0.14 ^{ab}	.04
CS 3-URO	42.7 \pm 27.4 ^y		0.19 \pm 0.14 ^{xy}	
T3 3-U	8.6 \pm 4.6 ^b	.67	0.12 \pm 0.04 ^{bc}	.51
T3 3-URO	10.0 \pm 9.1 ^y		0.14 \pm 0.08 ^{xy}	
T4 3-U	8.9 \pm 5.2 ^b	.56	0.22 \pm 0.12 ^{cd}	.86
T4 3-URO	10.5 \pm 6.7 ^y		0.22 \pm 0.08 ^y	

PS: Primescan, CS: CS 3600, T3: Trios 3, T4: Trios4, 3-U: 3 units (length of restoration), 3-URO: 3 units with reference objects, a,b,c,d: The different letters show statistically significant differences between 3-U group within each column. x,y: The different letters show statistically significant differences between the 3-URO group within each column.

**P* < .05

values were observed in CS (200.5 \pm 96.4), followed by T3 (15.5 \pm 7.6), PS (12.9 \pm 8.7), and T4 (12.5 \pm 6.9), respectively. Only the differences between CS and PS (*P* = .003), CS and T3 (*P* = .003), and CS and T4 (*P* = .003) were statistically significant. The presence of RO presented no statistically significant effect on the precision of distance values in 3-U models in any of the IOS devices (*P* > .05) (Table 3).

In terms of precision, the highest angle ($^{\circ}$) value in 4-U models was observed in CS (0.41 \pm 0.28), followed by T3 (0.13 \pm 0.07), T4 (0.09 \pm 0.07), and PS (0.03 \pm 0.02), respectively. Only the difference between CS and PS (*P* = .01), CS and T3 (*P* = .049), CS and T4 (*P* = .03), and PS and T3 (*P* = .01) were significant. With the involvement of RO, in 4-U models, the highest angle values were observed in CS (0.33 \pm 0.20), followed by T3 (0.14 \pm 0.19), T4 (0.10 \pm 0.06), and T4 (0.03 \pm 0.02), respectively. Only the differences between CS and PS (*P* = .007), CS and T4 (*P* = .02), PS and T3 (*P* = .03), and PS and T4 (*P* = .03) were statistically significant. The presence of RO presented no significant effect on the precision of angle values in 4-U models in any of the IOS devices (*P* > .05) (Table 3).

In terms of precision, the highest distance (μm) in 3-U models was observed in CS (108.7 \pm 68.2), followed by T4 (8.9 \pm 4.9), T3 (8.1 \pm 4.8), and PS (5.4 \pm 3.5), respectively. Only the difference between CS and

PS (*P* = .007), CS and T3 (*P* = .007), and CS and T4 (*P* = .008) were significant. With the involvement of RO, in 3-U models, the highest distance values were observed in CS (41.6 \pm 28.6), followed by T3 (9.7 \pm 9.3), T4 (6.1 \pm 3.7), and PS (3.8 \pm 61.2), respectively. Only the difference between CS and PS (*P* = .01), CS and T3 (*P* = .03), and CS and T4 (*P* = .02) were significant. Only in the CS group did the presence of RO present a statistically significant effect on distance values in 3-U models (*P* = .01), while the rest of the IOS performed similarly in the presence or absence of RO (*P* > .05) (Table 4).

In terms of precision, the highest angle ($^{\circ}$) value in 3-U models was observed in CS (0.33 \pm 0.14), followed by T4 (0.10 \pm 0.07), T3 (0.09 \pm 0.05), and PS (0.04 \pm 0.02), respectively. Only the difference between CS and PS (*P* = .003), CS and T3 (*P* = .004), and CS and T4 (*P* = .004) were statistically significant. With the involvement of RO, in 3-U models, the highest angle values were observed in CS (0.19 \pm 0.13), followed by T4 (0.07 \pm 0.05), T3 (0.06 \pm 0.05), and PS (0.03 \pm 0.02), respectively. Only the differences between CS and PS (*P* = .002) were statistically significant. Only in the CS group did the presence of RO present a statistically significant effect on distance values in 3-U models (*P* = .04), while the rest of the IOS performed similarly in the presence or absence of RO (*P* > .05) (Table 4).

Table 3. Precision of mean distance and angle values with their standard deviation in 4-unit models with or without RO with their respective *P* values

	Distance, μm mean \pm std	<i>P</i> *	Angle, $^\circ$ mean \pm std	<i>P</i> *
PS 4-U	17.5 \pm 9.6 ^b	.27	0.03 \pm 0.02 ^{cd}	.56
PS 4-URO	12.9 \pm 8.7 ^y		0.03 \pm 0.02 ^z	
CS 4-U	143.4 \pm 83.3 ^a	.17	0.41 \pm 0.28 ^a	.47
CS 4-URO	200.5 \pm 96.4 ^x		0.33 \pm 0.20 ^w	
T3 4-U	14.7 \pm 10.2 ^b	.86	0.13 \pm 0.07 ^b	.64
T3 4-URO	15.5 \pm 7.6 ^y		0.14 \pm 0.10 ^{wx}	
T4 4-U	15.3 \pm 8.1 ^b	.42	0.09 \pm 0.07 ^{bc}	.77
T4 4-URO	12.5 \pm 6.9 ^y		0.10 \pm 0.06 ^{xy}	

PS: Primescan, CS: CS 3600, T3: Trios 3, T4: Trios4, 4-U: 4 unit (length of restoration), 4-URO: 4 unit with reference objects, a,b,c: The different letters show statistically significant differences between 4-U group within each column. w,x,y,z: The different letters show statistically significant differences between the 4-URO group within each column.

**P* < .05

Table 4. Precision of mean distance and angle values with their standard deviation in 3-unit models with or without RO with their respective *P* values

	Distance, μm mean \pm std	<i>P</i> *	Angle, $^\circ$ mean \pm std	<i>P</i> *
PS 3-U	5.4 \pm 3.5 ^b	.20	0.04 \pm 0.02 ^b	.12
PS 3-URO	3.8 \pm 1.2 ^y		0.03 \pm 0.02 ^y	
CS 3-U	108.7 \pm 68.2 ^a	.01	0.33 \pm 0.14 ^a	.04
CS 3-URO	41.6 \pm 28.6 ^x		0.19 \pm 0.13 ^x	
T3 3-U	8.1 \pm 4.8 ^b	.63	0.09 \pm 0.05 ^b	.21
T3 3-URO	9.7 \pm 9.3 ^y		0.06 \pm 0.05 ^{xy}	
T4 3-U	8.9 \pm 4.9 ^b	.17	0.10 \pm 0.07 ^b	.22
T4 3-URO	6.1 \pm 3.7 ^y		0.07 \pm 0.05 ^{xy}	

PS: Primescan, CS: CS 3600, T3: Trios 3, T4: Trios4, 3-U: 3 unit (length of restoration), 3-URO: 3 unit with reference objects, a,b: The different letters show statistically significant differences between 3-U group within each column. x,y: The different letters show statistically significant differences between the 3-URO group within each column.

DISCUSSION

Diverse factors could impact the accuracy of digital scanning, which could explain the disparities observed among studies.¹³ Two of those variables were found to be highly effective: the length of the edentulous arch¹⁴ and the type of intraoral scanner equipment.¹⁵

According to the results of this study, in terms of trueness and precision of distance values, CS always presented significantly higher deviations compared to PS, while the other IOS devices presented variable

results in both 3-U and 4-U models. In terms of trueness and precision of angle values, CS always presented the highest deviation values, although the significance of those values compared to the other IOS devices varied among the groups in both 3-U and 4-U models. In CS 3-U models, the use of RO presented statistically significant differences in both trueness and precision of distance and angle values. In terms of trueness, the use of RO in PS groups created a statistically significant difference both in angle values of 4-U models and distance values of 3-U models. The use of RO presented no significant difference among

other IOS devices. Therefore, the first and second null hypotheses were both partially rejected, indicating that the type of the IOS device and the presence of RO might be co-dependent as an affecting factor on the accuracy of bite registration regardless of the length of the edentulous area.

According to a narrative review by Michelinakis *et al.*,¹⁶ intraoral scanning demonstrated high accuracy in models with both single and multiple implant applications. However, in the edentulous arches, no matter what the impression technique was, no significant difference between the intraoral scanner and the impression technique was observed.

In several articles, the trueness and precision of the digital scans obtained from the different IOS devices were evaluated by comparing them with scans obtained from a highly reliable laboratory scanner. Despite a notable distinction between the IOS and the fact that some of them exhibited greater accuracy while scanning the entire arch, none of the more recent IOS devices displayed a discrepancy in accuracy more than the anticipated 150 μm threshold.^{3,17-20} Every IOS performed differently in our investigation. As was consistent with earlier research, Primescan demonstrated significantly greater accuracy than CS 3600 and marginally better accuracy than the other evaluated IOS devices.²¹⁻²⁴ This might be due to the software algorithm of Primescan.²⁵ Digital scanners employ a digital language called STL to map out the surface of the scanned object by creating a triangular mesh.¹⁵ Different IOS devices employ different scanning methods, which results in variations in triangular mesh resolution and arrangement. These variations might impact the size of the triangles inside the mesh and, as a result, generate disparities in the 3D accuracy of the final product compared to the original subject.^{25,26}

For precise scan results, subsequent pictures must be precisely superimposed or stitched together. It is well known that this procedure results in dimensional disparities that are closely correlated with the inter-implant distance and the scanning scope. Research on partial arch digital scans has indicated that an increase in the inter-implant distance and the range of scans was associated with a decrease in the scanning accuracy.^{18,27-29} To overcome this problem, either the

use of auxiliary objects attached to the scan bodies³⁰ or interconnected scan bodies³¹ were suggested by different researchers. Motel *et al.*³² suggested the use of a single-step scanning process, including the implant position scans, instead of a two-step scanning process of the emergence profile and the implant position scans to increase the accuracy in partially edentulous arches. On the other hand, the use of internal or external implant connections was reported to have no influence on the scanning accuracy in completely edentulous arches.³³ In the present study, the use of reference objects created a statistically significant difference in the CS group, whereas no statistically significant difference was observed in any other IOSs. However, the usage of RO in partially edentulous areas accelerated the scanning process and stitching of digital images, so it can still be used as a helpful scanning measure, particularly on flexible soft tissues under clinical conditions.

In the current experiment, gingival imitation has been made of plastic, which has a dry, stiff, and inflexible matt texture. Consequently, the results of this study may vary under clinical conditions.

CONCLUSION

The type of intraoral scanner (IOS) influences the accuracy and consistency of digital scans in arches that are partially edentulous. Additionally, the application of reference objects (RO) generally enhances both the accuracy and consistency of digital scans, depending on the specific IOS device used, and this improvement is observed regardless of the length of the edentulous region. Further *in vivo* and *in vitro* research is needed to evaluate the advantages and limitations of RO.

REFERENCES

1. Papaspyridakos P, Vazouras K, Chen YW, Kotina E, Nato Z, Kang K, Chochlidakis K. Digital vs conventional implant impressions: a systematic review and meta-analysis. *J Prosthodont* 2020;29:660-78.
2. Wulfman C, Naveau A, Rignon-Bret C. Digital scanning for complete-arch implant-supported restorations: A systematic review. *J Prosthet Dent* 2020;124:161-7.

3. Rutkūnas V, Gečiauskaitė A, Jegelevičius D, Vaitiekūnas M. Accuracy of digital implant impressions with intraoral scanners. A systematic review. *Eur J Oral Implantol* 2017;10 Suppl 1:101-20.
4. Lin WS, Harris BT, Elathamna EN, Abdel-Azim T, Morton D. Effect of implant divergence on the accuracy of definitive casts created from traditional and digital implant-level impressions: an in vitro comparative study. *Int J Oral Maxillofac Implants* 2015;30:102-9.
5. Gimenez-Gonzalez B, Hassan B, Özcan M, Pradies G. An in vitro study of factors influencing the performance of digital intraoral impressions operating on active wavefront sampling technology with multiple implants in the edentulous maxilla. *J Prosthodont* 2017;26:650-5.
6. Stimmelmayer M, Güth JF, Erdelt K, Edelhoff D, Beuer F. Digital evaluation of the reproducibility of implant scanbody fit-an in vitro study. *Clin Oral Investig* 2012;16:851-6.
7. Ender A, Mehl A. Influence of scanning strategies on the accuracy of digital intraoral scanning systems. *Int J Comput Dent* 2013;16:11-21.
8. Mizumoto RM, Yilmaz B, McGlumphy EA Jr, Seidt J, Johnston WM. Accuracy of different digital scanning techniques and scan bodies for complete-arch implant-supported prostheses. *J Prosthet Dent* 2020;123:96-104.
9. Iturrate M, Eguiraun H, Solaberrieta E. Accuracy of digital impressions for implant-supported complete-arch prosthesis, using an auxiliary geometry part - An in vitro study. *Clin Oral Implants Res* 2019;30:1250-8.
10. Roig E, Roig M, Garza LC, Costa S, Maia P, Espona J. Fit of complete-arch implant-supported prostheses produced from an intraoral scan by using an auxiliary device and from an elastomeric impression: a pilot clinical trial. *J Prosthet Dent* 2022;128:404-14.
11. Rutkūnas V, Gedrimienė A, Al-Haj Husain N, Pletkus J, Barauskis D, Jegelevičius D, Özcan M. Effect of additional reference objects on accuracy of five intraoral scanners in partially and completely edentulous jaws: an in vitro study. *J Prosthet Dent* 2023;130:111-8.
12. Kim JE, Amelya A, Shin Y, Shim JS. Accuracy of intraoral digital impressions using an artificial landmark. *J Prosthet Dent* 2017;117:755-61.
13. Nuytens P, D'haese R, Vandeweghe S. Reliability and time efficiency of digital vs. analog bite registration technique for the manufacture of full-arch fixed implant prostheses. *J Clin Med* 2022;11:2882.
14. Lo Russo L, Ciavarella D, Salamini A, Guida L. Alignment of intraoral scans and registration of maxillo-mandibular relationships for the edentulous maxillary arch. *J Prosthet Dent* 2019;121:737-40.
15. Richert R, Goujat A, Venet L, Viguie G, Viennot S, Robinson P, Farges JC, Fages M, Ducret M. Intraoral scanner technologies: a review to make a successful impression. *J Healthc Eng* 2017;2017:8427595.
16. Michelinakis G, Apostolakis D, Kamposiora P, Papavasiliou G, Özcan M. The direct digital workflow in fixed implant prosthodontics: a narrative review. *BMC Oral Health* 2021;21:37.
17. Ender A, Mehl A. In vitro evaluation of the accuracy of conventional and digital methods of obtaining full-arch dental impressions. *Quintessence Int* 2015;46:9-17.
18. Fukazawa S, Odaira C, Kondo H. Investigation of accuracy and reproducibility of abutment position by intraoral scanners. *J Prosthodont Res* 2017;61:450-9.
19. Malik J, Rodriguez J, Weisbloom M, Petridis H. Comparison of accuracy between a conventional and two digital intraoral impression techniques. *Int J Prosthodont* 2018;31:107-13.
20. Chochlidakis K, Papaspyridakos P, Tsigarida A, Romeo D, Chen YW, Natto Z, Ercoli C. Digital versus conventional full-arch implant impressions: a prospective study on 16 edentulous maxillae. *J Prosthodont* 2020;29:281-6.
21. Ender A, Zimmermann M, Mehl A. Accuracy of complete- and partial-arch impressions of actual intraoral scanning systems in vitro. *Int J Comput Dent* 2019;22:11-9.
22. Passos L, Meiga S, Brigagão V, Street A. Impact of different scanning strategies on the accuracy of two current intraoral scanning systems in complete-arch impressions: an in vitro study. *Int J Comput Dent* 2019;22:307-19.
23. Son K, Jin MU, Lee KB. Feasibility of using an intraoral scanner for a complete arch digital scan, part 2: a comparison of scan strategies. *J Prosthet Dent* 2023;129:341-9.
24. Diker B, Tak Ö. Accuracy of six intraoral scanners for scanning complete-arch and 4-unit fixed partial dentures: an in vitro study. *J Prosthet Dent* 2022;128:187-94.

25. Ender A, Zimmermann M, Attin T, Mehl A. In vivo precision of conventional and digital methods for obtaining quadrant dental impressions. *Clin Oral Investig* 2016;20:1495-504.
26. Zimmermann M, Koller C, Rumetsch M, Ender A, Mehl A. Precision of guided scanning procedures for full-arch digital impressions in vivo. *J Orofac Orthop* 2017;78:466-71.
27. Imburgia M, Logozzo S, Hauschild U, Veronesi G, Mangano C, Mangano FG. Accuracy of four intraoral scanners in oral implantology: a comparative in vitro study. *BMC Oral Health* 2017;17:92.
28. Flügge TV, Att W, Metzger MC, Nelson K. Precision of dental implant digitization using intraoral scanners. *Int J Prosthodont* 2016;29:277-83.
29. Kim JE, Hong YS, Kang YJ, Kim JH, Shim JS. Accuracy of scanned stock abutments using different intraoral scanners: an in vitro study. *J Prosthodont* 2019;28:797-803.
30. Iturrate M, Eguiraun H, Etxaniz O, Solaberrieta E. Accuracy analysis of complete-arch digital scans in edentulous arches when using an auxiliary geometric device. *J Prosthet Dent* 2019;121:447-54.
31. Huang R, Liu Y, Huang B, Zhang C, Chen Z, Li Z. Improved scanning accuracy with newly designed scan bodies: an in vitro study comparing digital versus conventional impression techniques for complete-arch implant rehabilitation. *Clin Oral Implants Res* 2020;31:625-33.
32. Motel C, Kirchner E, Adler W, Wichmann M, Matta RE. Impact of different scan bodies and scan strategies on the accuracy of digital implant impressions assessed with an intraoral scanner: an in vitro study. *J Prosthodont* 2020;29:309-314.
33. Alikhasi M, Siadat H, Nasirpour A, Hasanzade M. Three-dimensional accuracy of digital impression versus conventional method: effect of implant angulation and connection type. *Int J Dent* 2018;2018:3761750.